Laukkanen, Olli-Ville; Winter, H. Henning; Soenen, Hilde; Seppälä, Jukka

An empirical constitutive model for complex glass-forming liquids using bitumen as a model material

Published in:
Rheologica Acta

DOI:
10.1007/s00397-017-1056-6

Published: 01/01/2018

Document Version
Peer reviewed version

Published under the following license:
Unspecified

Please cite the original version:
Laukkanen, O-V., Winter, H. H., Soenen, H., & Seppälä, J. (2018). An empirical constitutive model for complex glass-forming liquids using bitumen as a model material. *Rheologica Acta*, *57*(1), 57-70. https://doi.org/10.1007/s00397-017-1056-6

An empirical constitutive model for complex glass-forming liquids using bitumen as a model material

Olli-Ville Laukkanen[1,2], H. Henning Winter[1], Hilde Soenen[3], and Jukka Seppälä[2]

[1] Department of Polymer Science and Engineering and Department of Chemical Engineering, University of Massachusetts, Amherst, Massachusetts 01003, United States

[2] Department of Chemical and Metallurgical Engineering, School of Chemical Technology, Aalto University, P.O. Box 16100, 00076 Aalto, Finland

[3] Nynas NV, 2000 Antwerp, Belgium

Abstract While extensive research efforts have been devoted to understand the dynamics of chemically and structurally simple glass-forming liquids (SGFLs), the viscoelasticity of chemically and structurally complex glass-forming liquids (CGFLs) has received only little attention. This study explores the rheological properties of CGFLs in the vicinity of the glass transition. Bitumen is selected as the model material for CGFLs due to its extremely complex chemical composition and microstructure, fast physical aging and thermorheological simplicity, and abundant availability. A comprehensive rheological analysis reveals a significant broadening of the glass transition dynamics in bitumen as compared to SGFLs. In particular, the relaxation time spectrum of bitumen is characterized by a broad distribution of long relaxation modes. This observation leads to the development of a new constitutive equation, named the broadened power-law spectrum model. In this model, the wide distribution of long relaxation times is described by a power-law with positive exponent and a stretched exponential cut-off, with parameter β serving as a measure of the broadness of the distribution. This characteristic shape of the bitumen spectrum is attributed to the heterogeneous freezing of different molecular components of bitumen, i.e. to the coexistence of liquid and glassy micro-phases. Furthermore, as this type of heterogeneous glass transition behavior can be considered as a general feature of complex glass-forming systems, the broadened power-law spectrum model is expected to be valid for all types of CGFLs. Examples of the applicability of this model in various complex glass-forming systems are given.

Keywords: Glass transition; Glass-forming liquids; Linear viscoelasticity; Relaxation time spectrum; Bitumen

Introduction

Dynamics of molecular glass-forming liquids (GFLs) have been a subject of intense research over the past five decades or so (Angell et al. 2000; Bengtzelius et al. 1984; Böhmer et al. 1993; Donth 2001; Dyre 2006; Götze and Sjögren 1992; Götze 1999; Hansen et al. 1997; Hansen et al. 1998; Richert and Angell 1998; Stickel et al. 1995; Stickel et al. 1996). The most important experimental techniques in this field are rheology (Le Bourhis 2008) and dielectric spectroscopy (Lunkenheimer et al. 2000). However, despite extensive research efforts, the

theory of glass dynamics remains somewhat elusive (Hecksher et al. 2008; McKenna 2008). This is partly due to the fact that the fundamentals of the glass transition itself are still far from being understood (Langer 2007). Furthermore, dynamic mechanical measurements in the glassy state are demanding due to physical aging effects (McKenna 2012), significantly reducing the amount of experimental data available for developing a quantitative understanding of the equilibrium dynamics of glass-forming systems. Physical aging is caused by trapped non-equilibrium structured states which slowly recover. This impacts the mechanical material response, persisting up to thousands or even millions of years in various types of glassy materials (Struik 1977).

Since the linear viscoelastic behavior of any material can be fully described by its relaxation modulus $G(t)$ or relaxation time spectrum $H(\tau)$, it is desirable to develop constitutive equations that describe one of these functions. Perhaps the most popular model for describing the linear dynamics of GFLs is the Kohlrausch-Williams-Watts (KWW) function – originating from the work of Kohlrausch (1854) and Williams and Watts (1970) – that assumes a stretched exponential form for the relaxation modulus (Berry and Plazek 1997; Ngai et al. 1997):

$$G(t) = G_g e^{-(t/\tau_{KWW})^{\beta_{KWW}}} \tag{1}$$

where G_g is the glassy modulus, τ_{KWW} is the characteristic relaxation time, and β_{KWW} is a stretching parameter related to the breadth of the relaxation time spectrum. The KWW function has been generally found to provide a reasonable description of the relaxation response of many polymeric and small-molecule glass formers. More recently, Winter and coworkers (2009; 2013) discovered that the relaxation in many molecular and colloidal glasses can be closely expressed with a power-law relaxation time spectrum:

$$H(\tau, \varepsilon) = n_\alpha G_c \left(\frac{\tau}{\tau_\alpha(\varepsilon)}\right)^{n_\alpha}, \quad \text{for } \tau < \tau_\alpha(\varepsilon) \text{ and } n_\alpha \geq 0 \tag{2}$$

where ε is the distance from the glass, n_α is a positive-valued exponent that originates from the mode coupling theory (MCT), G_c is the plateau modulus of the G' data, and τ_α is the longest relaxation time. It is worth noting that Winter's power-law spectrum model is identical to the Baumgaertel-Schausberger-Winter (BSW) model (1990) without contributions from the β-relaxation.

The possible shortcoming of the KWW and power-law spectrum models, however, is that their validity has been tested adequately only for simple glass-forming liquids (SGFLs). Here we define SGFLs to be materials that are both molecularly and excitationally simple, following the definitions established by Angell et al. (1999). This is different for complex glass-forming liquids (CGFL), which are composed of a broad range of molecules with diverse intramolecular and intermolecular interactions. The viscoelasticity of CGFLs has received little attention. This is rather surprising as CGFLs can be found in Nature and are widely used in industrial applications.

In order to narrow this knowledge gap, we perform an experimental rheological study using bitumen as a model CGFL. The advantages of bitumen as model material are:

- Bitumen is known to be both compositionally and structurally complex material. It is an extremely broad mixture of substantially different molecules, namely oligomeric hydrocarbons with small amounts of sulfur, nitrogen and oxygen and traces of metals like vanadium and nickel (Lesueur 2009; Redelius and Soenen 2015). These interact in many different ways locally and long range. Molecular interactions include dispersive, polar, hydrogen bonding and π-π interactions (Redelius and Soenen 2015). Notably, it has been shown that the rheological properties of bitumen are largely determined by aromatic interactions (Redelius and Soenen 2015; Soenen and Redelius 2014; Soenen et al. 2016) and by the content of carbonyl and sulfoxide functional groups (Qin et al. 2014).
- The glass transition temperature of bitumen (typically $T_g \approx$ -20 °C) is relatively high when comparing to many other low-molecular-weight GFLs. This makes the glassy state of bitumen very accessible, even for commercial rheometers with standard temperature control systems.
- Physical aging is relatively fast in non-waxy bitumen, even well below T_g, making it possible to perform rheological experiments in the "equilibrium" glassy state within a practical timeframe. This will be experimentally demonstrated in Section "Physical aging in bitumen".
- Bitumen is readily available and widely used in various industrial applications such as in asphalt paving.

Consequently, bitumen can be considered as a CGFL that is ideal for the purposes of this study. It should be pointed out, however, that the chemical composition and rheological properties of bitumen are highly dependent on its crude oil source and refining methods. In this way, bitumen cannot be considered as a well-defined model material in the usual meaning of this term. Nevertheless, as our analysis focuses on rheological properties that are believed to be characteristic for CGFLs in general, this is not a major drawback in terms of the scope of this study.

In this research, we first determine linear viscoelastic properties of bitumen during physical aging and in the aged state, near and below the glass transition temperature. Then, the rheological response of bitumen is compared to that of SGFLs in the vicinity of the glass transition and distinct differences are demonstrated. These observations lead to the development of a new constitutive model for CGFLs based on the relaxation time spectrum of bitumen. We attempt a physical interpretation of CGFL phenomena and explore a wider applicability of the proposed constitutive model. In addition, a comparison is performed with the existing models for glassy relaxation.

Experimental

The bitumen sample used in this investigation is a vacuum residue obtained from the distillation of Venezuelan crude oil. Basic properties of the bitumen sample are given in Table 1. The heat flow curve of the bitumen and its temperature derivative, as measured by a Mettler Toledo DSC1 differential scanning calorimeter, are presented in Fig. 1. These DSC data

demonstrate the very broad glass transition of the bitumen, spanning over a temperature range of several tens of Kelvin. The absence of endothermic peaks indicates that the bitumen sample does not contain any crystallizable fractions (paraffinic waxes), i.e. it can be considered to be completely amorphous. The nominal glass transition temperature, T_g, of the bitumen was determined as -20 °C.

Table 1 Basic properties of the investigated bitumen sample.

Property	Standard/method	Measured value
Needle penetration at 25 °C [dmm]	EN 1426	64
Ring-and-Ball softening point [°C]	EN 1427	47.7
Performance grade	AASHTO M320	PG 64-22
SARA fractions	Iatroscan TLC/FID [a]	
Saturates [wt%]		6
Aromatics [wt%]		51
Resins [wt%]		23
Asphaltenes [wt%]		20
Molecular weight properties	Gel permeation chromatography [b]	
M_n [g/mol]		1053
M_w [g/mol]		2320
M_w/M_n [-]		2.20

[a] The TLC-FID method used in this study is similar to the one described in the IP-469 standard.
[b] Gel permeation chromatography was performed on 0.8 % tetrahydrofuran solutions of bitumen using an Alliance 2690 Separator with a differential refractometer (RI) detector and a Waters 996 photo diode array (PDA) detector calibrated with narrow polystyrene standards. However, as emphasized by Soenen and Redelius (2014), molecular weights determined for bitumen by GPC are only directional, and therefore the values reported in this table should be considered as mere approximates.

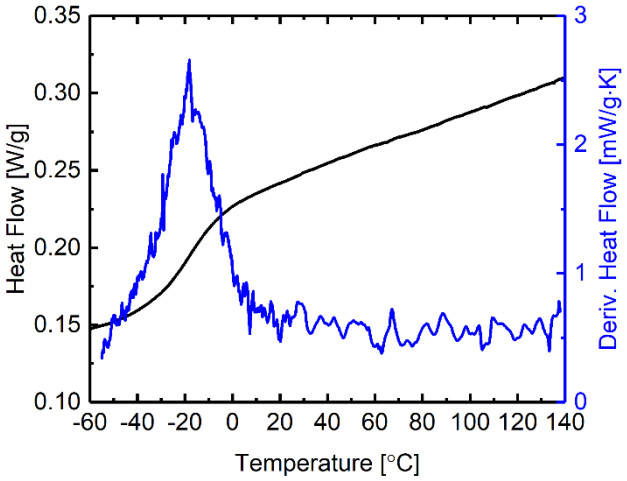

Fig. 1 The heat flow curve of the investigated bitumen and its temperature derivative measured at a heating rate of 10 K/min.

Rheological experiments were performed using a stress-controlled Malvern Kinexus Pro rheometer. A Peltier plate and active hood provide an accurate and gradient-free temperature control, in conjunction with a Julabo CF41 refrigerated circulator, which served as a heat exchanger to remove heat formed in the Peltier temperature control system. All rheological experiments were performed in an N_2 environment to avoid moisture uptake and ice formation in the test specimen. Small-diameter parallel plate (SDPP) rheometry (4-mm plate diameter and 1.75-mm gap) was employed to minimize torsional instrument compliance effects caused by high sample stiffness. Details of the SDPP rheometry have been described by Laukkanen (2017), demonstrating the practicality and excellent repeatability of this measurement technique. All measured rheological data were corrected for instrument compliance, J_i, according to Eqs. (3)-(5) (Laukkanen 2017; Marin 1988):

$$G'_s = \frac{G'_m\left(1-\frac{J_\mathrm{i}}{k_g}G'_m\right)-\frac{J_\mathrm{i}}{k_g}G''^{2}_m}{\left(1-\frac{J_\mathrm{i}}{k_g}G'_m\right)^2+\left(\frac{J_\mathrm{i}}{k_g}G''_m\right)^2} \tag{3}$$

$$G''_s = \frac{G''_m}{\left(1-\frac{J_\mathrm{i}}{k_g}G'_m\right)^2+\left(\frac{J_\mathrm{i}}{k_g}G''_m\right)^2} \tag{4}$$

$$\tan\delta_s = \frac{G''_s}{G'_s} = \frac{G''_m}{G'_m\left(1-\frac{J_\mathrm{i}}{k_g}G'_m\right)-\frac{J_\mathrm{i}}{k_g}G''^{2}_m} \tag{5}$$

where G'_s, G''_s, and tan δ_s denote the true (compliance corrected) values of the storage modulus, loss modulus and loss tangent of the sample, respectively, G'_m and G''_m are the measured values, and k_g is the geometry conversion factor (for the parallel plate geometry, $k_g = 2h / \pi R^4$, where h is the gap between the plates of radius R). The torsional compliance of the rheometer setup in this study, $J_i = 0.00964$ rad/Nm, was determined experimentally as outlined in Fig. S1 of the Supplementary Material.

Isothermal frequency sweep measurements (f = 10 … 0.01 Hz) were performed at various temperatures ranging from 10 to -40 °C in 10 K intervals. Strain amplitudes were kept small (γ_0 = 0.075 … 0.01 % depending on the measurement temperature, see Table S1 of the Supplementary Material for details) in order to remain in the linear viscoelastic regime. Normal force control was used to automatically adjust the measurement gap near and below the nominal glass transition temperature in order to avoid the build-up of normal forces in the test specimen while maintaining good adhesion between the plates and the specimen.

The physical aging properties of bitumen were characterized by means of time-resolved rheometry experiments (Mours and Winter 1994). Isothermal cyclic frequency sweep (ICFS) measurements were performed to monitor the time evolution in the linear viscoelastic properties quasi-simultaneously at various angular frequencies (f = 10 … 0.1 Hz). ICFS experiments were performed at various temperatures between 10 °C (T_g+30 K) and -40 °C (T_g-20 K). Prior to each measurement, the bitumen specimen was quenched at approximately 10 K/min from 30 °C (well above the T_g) to the respective measurement temperature. The strain

amplitude was kept low (γ_0 = 0.03 … 0.01 % depending on the measurement temperature, see Table S1 of the Supplementary Material for details) in order to not disturb the physical aging process, and the normal force control was employed in the same way as described above. ICFS data were collected for at least 20 hours at each measurement temperature.

Rheological data of SGFLs retrieved from the literature

For comparison purposes, rheological data of selected SGFLs were retrieved from the literature and analyzed. Information of these data sets is summarized in Table 2.

Table 2 Rheological data sets of SGFLs analyzed in this study.

Source of data	Material	T_g [°C]	Measurement method	Reference
McKenna group (Texas Tech)	sucrose benzoate	62	8-mm diameter parallel plates with instrument compliance corrections (Schröter et al. 2006)	(Hutcheson and McKenna 2008)
	m-toluidine	-87		
	glycerol	-82		
Schröter & Donth (Univ. Halle)	glycerol	-82	Hyperbolically shaped sample between 8-mm diameter parallel plates (Plazek and Magill 1966)	(Schröter and Donth 2000)
Glass & Time group (Roskilde Univ.)	tetraphenyl-tetramethyl-trisiloxane (DC704)	-63	Self-built piezoelectric shear-modulus gauge (PSG) (Christensen and Olsen 1995) + self-built cryostat and temperature control system (Igarashi et al. 2008)	(Hecksher et al. 2013)
	1,2-propanediol	-109		(Maggi et al. 2008)
	pentaphenyl-trimethyl-trisiloxane (DC705)	-49		
Mills (Inst. für Silicatforschung, Würzburg)	soda-silica glass (Na_2O:2SiO_2)	455	Rod-shaped sample measured with a torsion tester	(Mills 1974)

Results

Physical aging in bitumen

Since rheological experiments on glassy materials are meaningful only if the material has been physically aged into equilibrium after sufficiently long times, ICFS experiments were performed to quantify the extent of physical aging in the investigated bitumen sample. Figure 2 shows data obtained from ICFS experiments at selected temperatures. Part (a) of this figure shows ICFS data measured at the nominal T_g of the bitumen (-20 °C); this is the temperature at which the rate of physical aging is typically at its highest in bitumen (Tabatabaee et al. 2012). It can be observed that, due to physical aging, the storage modulus (G') increases and the loss modulus (G'') decreases slightly at short aging times. However, already after a few hours physical aging practically ceases and G' and G'' (and also all other rheological parameters not plotted here) become almost time-independent.

It is also necessary to study physical aging well below T_g, as it is well known that physical aging persists the longer the further below T_g the material is aged (McKenna 2012). Part (b) of Fig. 2 presents ICFS data measured 20 K below the nominal T_g of the bitumen, i.e. at -40 °C. Similar observations can be made as above: physical aging has only moderate impact on the linear viscoelastic properties and it practically completes in less than ten hours. Therefore, we can conclude that bitumen practically reaches its equilibrium state within the timeframe of our rheological experiments. This means that the rheological data reported in the following sections are only insignificantly, if at all, affected by physical aging.

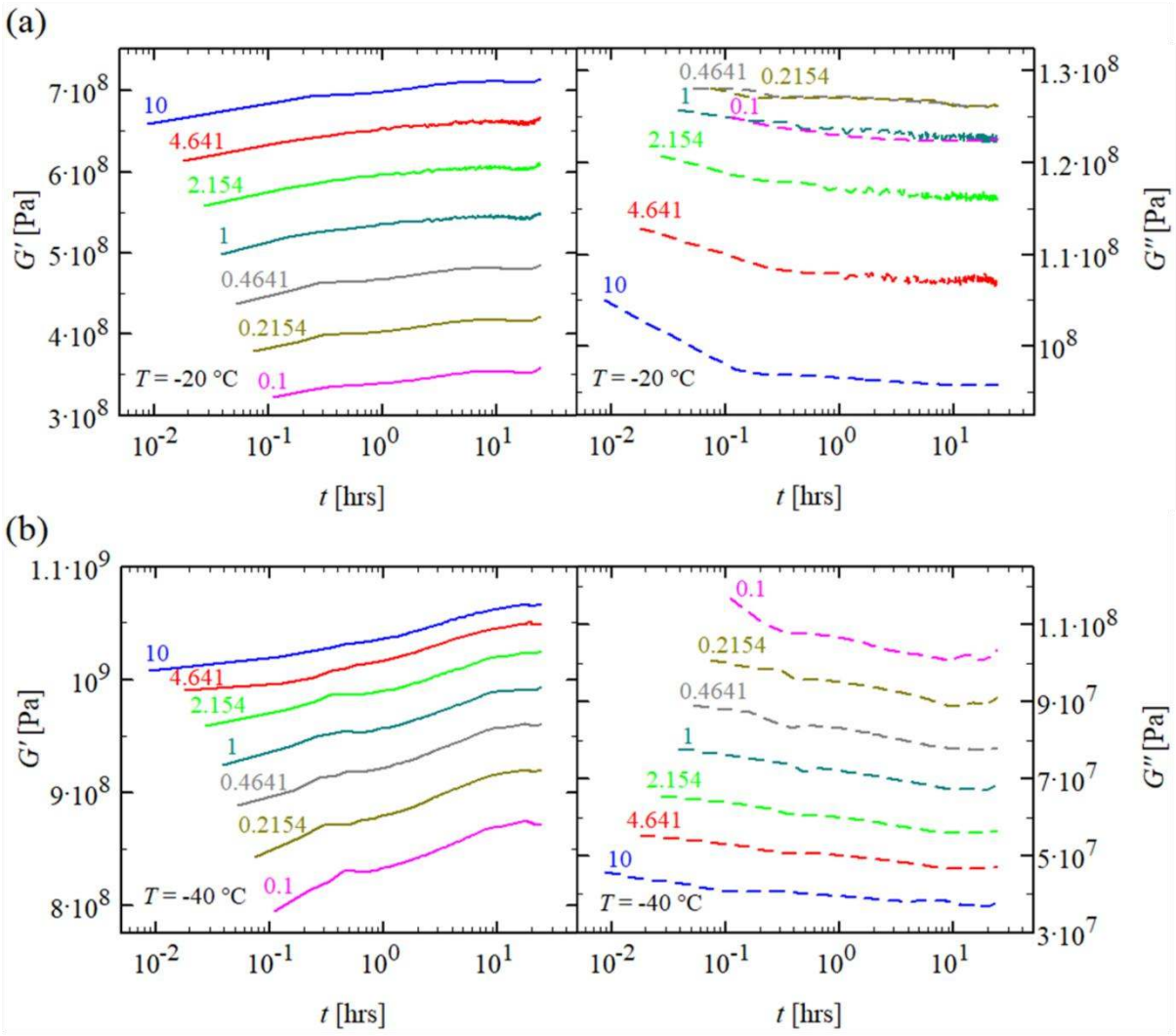

Fig. 2 ICFS data measured during the physical aging of the bitumen (a) at the nominal T_g and (b) 20 K below the nominal T_g. The figures near the curves denote the measurement frequency in Hz. For clarity, lines are used to present discrete data.

Linear viscoelasticity of bitumen near and below the glass transition

Before proceeding to the development of a new constitutive equation for bitumen and other CGFLs, it is necessary to investigate the applicability of the time-temperature

superposition principle (TTSP) near and below T_g. Fig. 3 shows frequency sweep data for bitumen at various temperatures in the plot of loss angle versus log|G^*|. This diagram is commonly known as the van Gurp-Palmen plot (van Gurp and Palmen 1998) or the Booij-Palmen plot (Booij and Palmen 1992), and it is particularly suitable for detecting thermorheological complexity, i.e. a failure of TTSP (Dealy and Plazek 2009; Stadler et al. 2015). In the case of bitumen, the frequency sweep data measured at different temperatures appear to superimpose, indicating thermorheological simplicity.

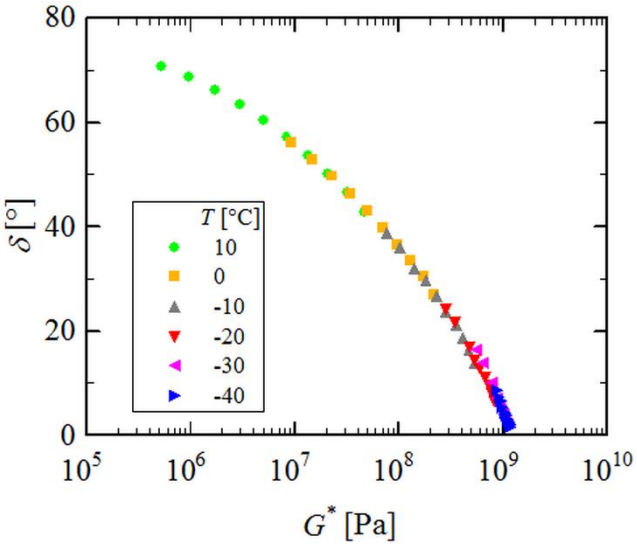

Fig. 3 Booij-Palmen plot of the bitumen.

However, when this same data set is depicted in the Cole-Cole plot, i.e. in the plot of G'' versus G' (Friedrich and Braun 1992), the isothermal frequency sweep curves do not perfectly superimpose (Fig. 4a). This is due to the linearly scaled axes of the Cole-Cole plot, as this representation magnifies the high-modulus part of the data. Consequently, even slight discrepancies in the overlap of the low-temperature frequency sweep curves become visible. The same type of approach has been used by Hecksher et al. (2013) to detect thermorheological complexity in some other GFLs. Nevertheless, even though the frequency sweep curves in Fig. 4a show discrepancy, bitumen can be considered as thermorheologically simple material. This is because these curves can be merged with the use of modulus shifts b_T, also known as vertical shifts (Fig. 4b). The magnitude of these modulus shifts is discussed more in detail later in this section.

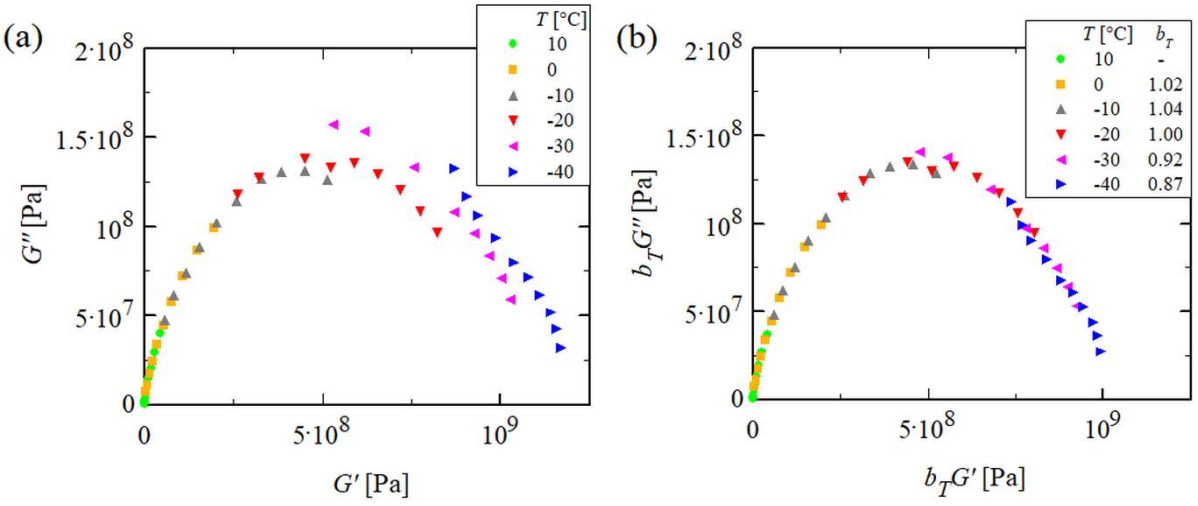

Fig. 4 Cole-Cole plots of the bitumen (a) without and (b) with modulus shifts applied.

It is well known that different types of bitumen often exhibit thermorheologically complex behavior due to the presence of a temperature-dependent structure for the asphaltene particles and melting/crystallization of the crystalline waxes naturally present in some bitumens (Lesueur et al. 1996; Lesueur 1999). However, in some special cases, thermorheologically simple behavior may be observed in non-waxy, low-asphaltene-content bitumens. The thermorheological simplicity of the investigated bitumen sample is confirmed by the overlap of frequency sweep data in the Booij-Palmen plot, see Fig. S2 of the Supplementary Material. Owing to the thermorheological simplicity, master curves of linear dynamic viscoelastic properties can be generated for this material. Fig. 5 shows master curves of *G'*, *G''* and tan δ that were constructed by using both time (horizontal) shifts a_T and modulus (vertical) shifts b_T. The master curves reflect typical rheological characteristics of a low-molecular-weight viscoelastic liquid; there is a direct transition from the terminal flow region into the glassy region without intermediate entanglement plateau. In the glassy regime, *G'* attains values close to 1 GPa, similarly to many other GFLs (Donth 2001).

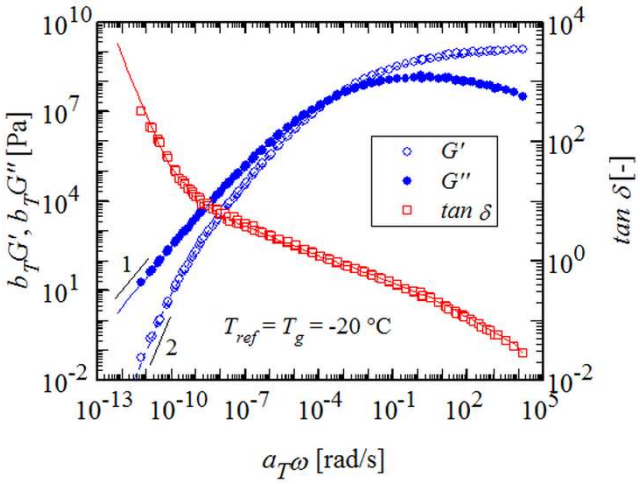

Fig. 5 Linear viscoelastic master curves for the bitumen. Note that high-temperature dynamic rheological data measured for this sample by Soenen and Redelius (2014) is used to extend the

master curves to lower frequencies where $G'(\omega)$ and $G''(\omega)$ display the terminal slopes of 2 and 1, respectively. The lines correspond to the fit of the generalized Maxwell model.

The temperature shift factors a_T and b_T used to construct the master curves of Fig. 5 are plotted in Fig. 6. It is observed that the temperature dependence of a_T includes an inversion point as can be described by the modified Kaelble equation (Rowe and Sharrock 2011):

$$\log a_T = -c_1 \left(\frac{T - T_d}{c_2 + |T - T_d|} - \frac{T_{ref} - T_d}{c_2 + |T_{ref} - T_d|} \right) \tag{6}$$

where c_1 and c_2 are fitting parameters, T_d is the defining temperature at which the curvature of the shift factor curve changes, and T_{ref} is the reference temperature. As opposed to the classical Williams-Landel-Ferry (WLF) equation, this shift factor function suggests non-diverging time scales at a finite temperature below T_g. This prediction of non-diverging time scales is in agreement with several recent theoretical and experimental studies (Elmatad et al. 2009; Elmatad et al. 2010; Mauro et al. 2009; McKenna 2008; McKenna 2009; McKenna and Zhao 2015; Pazmiño Betancourt et al. 2014; Zhao et al. 2013). In comparison to time shift factors a_T, modulus shift factors b_T are close to unity. For macromolecular materials modulus shifts result from temperature-induced density changes (Ferry 1980):

$$b_T = \frac{T_{ref}\rho(T_{ref})}{T\rho(T)} \tag{7}$$

where $\rho(T_{ref})$ is the density of the material at T_{ref} and $\rho(T)$ is the density at T. Bitumen is of low molecular weight and Eq. (7) might not apply. In spite of that, the experimentally determined b_T values are of the same order of magnitude as the b_T values predicted by Eq. (7).

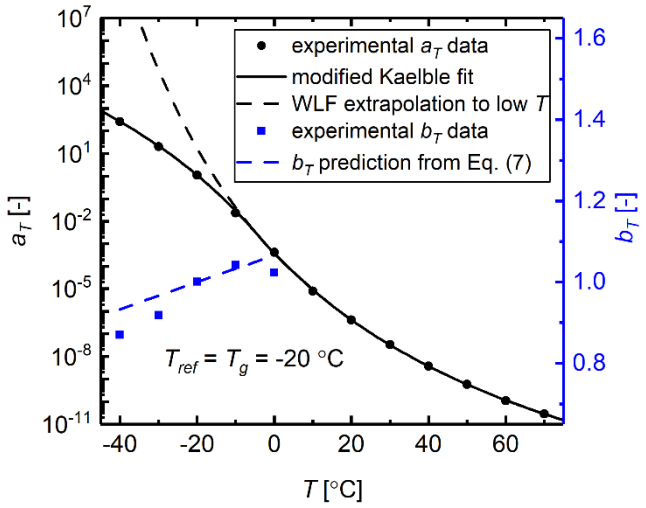

Fig. 6 Time (horizontal) shift factors a_T and modulus (vertical) shift factors b_T used to construct the master curves of Fig. 5. Note that modulus shifts are not necessary at temperatures well above T_g and that the scales are different for a_T and b_T. The solid black line corresponds to the fit of the modified Kaelble equation, Eq. (6), to the experimental a_T data, the dashed black line

corresponds to the extrapolation of the WLF equation to temperatures near and below T_g, and the dashed blue line corresponds to the b_T values predicted by Eq. (7). The parameter values for the modified Kaelble fit are c_1 = 17.2, c_2 = 86.2 K, T_d = 268.8 K. The prediction of Eq. (7) assumes the volumetric thermal expansion coefficient of bitumen to be 0.00061 K^{-1} (Eschrich 1980).

Comparison of the linear viscoelastic behavior of bitumen and SGFLs

According to the scope of this article, rheological characteristics of bitumen are compared with those of SGFLs in the vicinity of the glass transition. A simple comparison can be performed, for example, by plotting the linear viscoelastic dynamic data of these materials in the reduced Booij-Palmen plot (Fig. 7). In this plot, the bitumen curve is observed to have a much broader shape than the curves of the SGFLs, demonstrating an unusually gradual transition from the liquid state (where δ approaches 90°) into the glassy state (where δ approaches 0°) in bitumen. As will be described more fully below, this type of broadening of the glass transition dynamics is not expected to be unique to bitumen, but is believed to be a general feature of CGFLs.

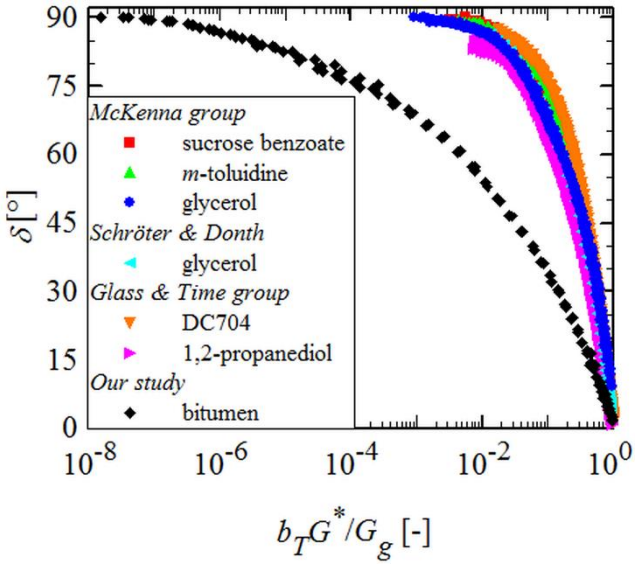

Fig. 7 Comparison of the linear viscoelastic properties of bitumen and selected SGFLs in the reduced Booij-Palmen plot. Modulus shifts b_T are used to generate smooth curves, and the modulus data are normalized with respect to the glassy modulus G_g to allow easier comparison of the shapes of the curves. The b_T and G_g values of the different materials are listed in Table S2 of the Supplementary Material.

Similarly, the shapes of the master curves reflect the broadening of the glass transition dynamics in bitumen. This is demonstrated in Fig. 8 where the shapes of the master curves of bitumen and selected SGFLs are compared. In particular, it is observed that the KWW function, Eq. (1), fits well to the master curves of all investigated SGFLs (Fig. S3 of the Supplementary Material), but not to the broad master curves of bitumen (Fig. 9). This observation provides evidence that the KWW function is not valid for CGFLs. Some evidence of the inability of the

KWW function to describe the rheological properties of bitumen has also been provided by Zanzotto and Stastna (1997).

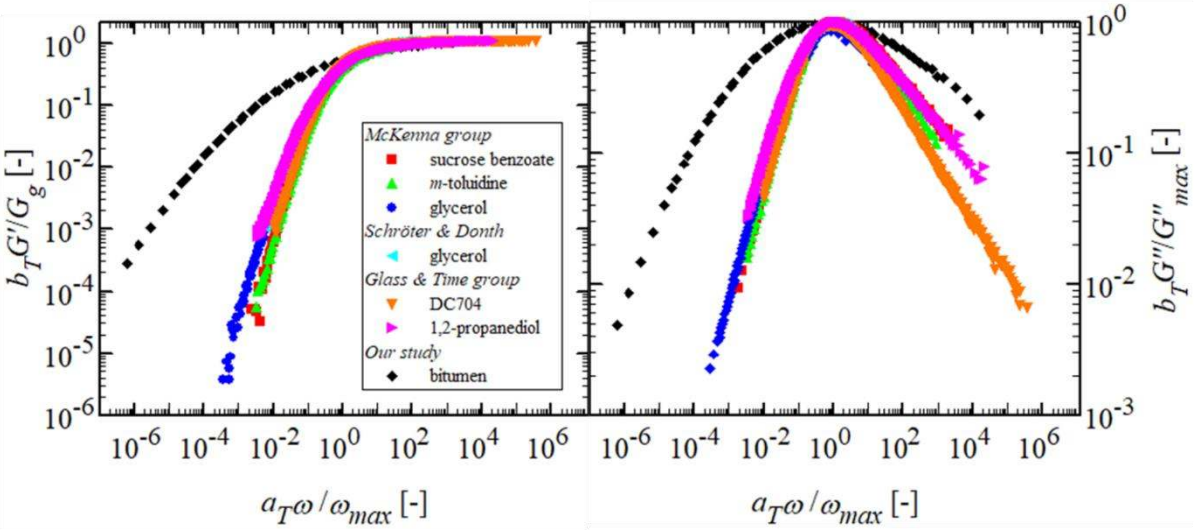

Fig. 8 Reduced storage modulus (left panel) and loss modulus (right panel) master curves of bitumen and selected SGFLs. The frequency axis is normalized with respect to the angular frequency corresponding to the maximum in *G''*. The *G'* values are normalized with respect to the glassy modulus G_g and the *G''* values are normalized with respect to the maximum in *G''* to allow easier comparison of the shapes of the curves.

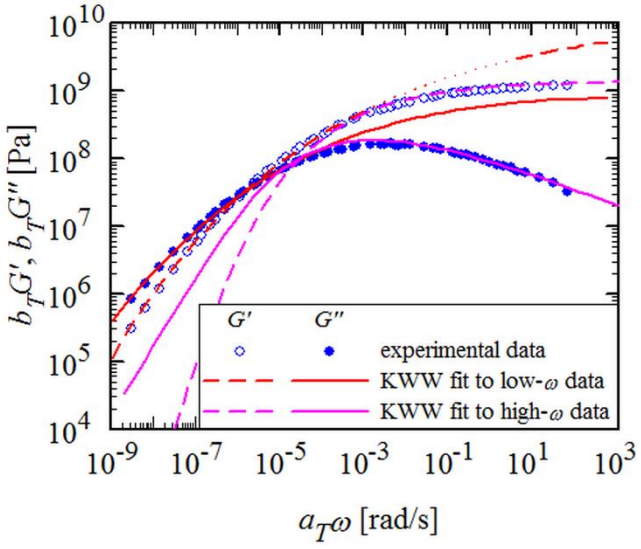

Fig. 9 Unsuccessful attempts to fit the KWW function to the dynamic moduli data of bitumen in the vicinity of the glass transition. The parameter values for the low-frequency fit are $G_g = 1.45\times10^{10}$ Pa, $\tau_{KWW} = 7.94\times10^{-4}$ s, $\beta_{KWW} = 0.09$, and for the high-frequency fit $G_g = 1.35\times10^{9}$ Pa, $\tau_{KWW} = 3.98\times10^{2}$ s, $\beta_{KWW} = 0.24$.

Relaxation time spectra of the investigated SGFLs and bitumen were calculated from their respective dynamic moduli master curves using the method of Baumgaertel and Winter (1989; 1992). As proposed by Winter (2013), all SGFLs are found to exhibit a power-law

spectrum with a positive power-law exponent and a sharp cut-off at the longest relaxation time, Eq. (2) (Fig. 10). On the contrary, the bitumen spectrum is characterized by a broad distribution of relaxation times at long times, which can be attributed again to the characteristic broadening of the glass transition dynamics. It is therefore obvious that the power-law spectrum model of Eq. (2) cannot be used to characterize the dynamics of CGFLs, thus justifying the need for the development of a new constitutive model.

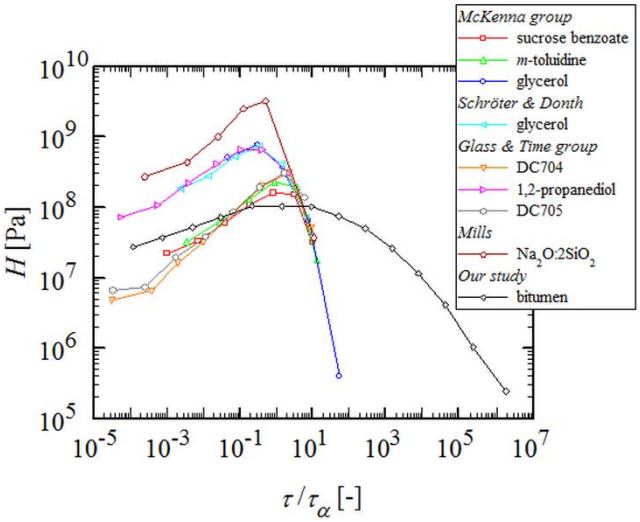

Fig. 10 Comparison of the relaxation time spectra of bitumen and SGFLs. The relaxation times are normalized with respect to the maximum relaxation time to allow easier comparison of the shapes of the curves.

New constitutive model for CGFLs

It is clear from Fig. 10 that the short time part of the bitumen spectrum can, similarly to the spectra of SGFLs, be described by a power-law equation with a positive exponent. However, as pointed out above, the power-law spectrum model of Eq. (2) is not able to describe the long relaxation time modes of bitumen. We suggest that the broad distribution of long relaxation times can be conveniently described by terminating the power-law spectrum with a stretched exponential function. Therefore, the relaxation time spectrum of bitumen may be expressed by the following equation:

$$H(\tau) = n_\alpha G_c \left(\frac{\tau}{\tau_\alpha}\right)^{n_\alpha} \exp\left[-\left(\frac{\tau}{\tau_\alpha}\right)^{\beta}\right], \quad \text{for } \beta < 1 \text{ and } 0 < n_\alpha \leq 1 \tag{8}$$

where β is a stretching parameter that describes the broadening of the relaxation time spectrum at long relaxation times. Note that Eq. (8) is identical to Eq. (2) with the addition of the stretched exponential term. We shall call Eq. (8) the broadened power-law spectrum model. An excellent fit of this model to the relaxation time spectrum of bitumen is shown in Fig. 11a. In addition, Fig. 11b depicts the corresponding model fits to the dynamic moduli data of bitumen. It is evident that these fits are superior to the KWW fits presented in Fig. 9, providing further proof of the successful applicability of this new model. Note that the *G'* and *G''* fits of

Fig. 11b were calculated using the numerical discretization scheme of Winter and Mours (2006) since these material functions cannot be analytically derived from the broadened power-law spectrum model, Eq. (8).

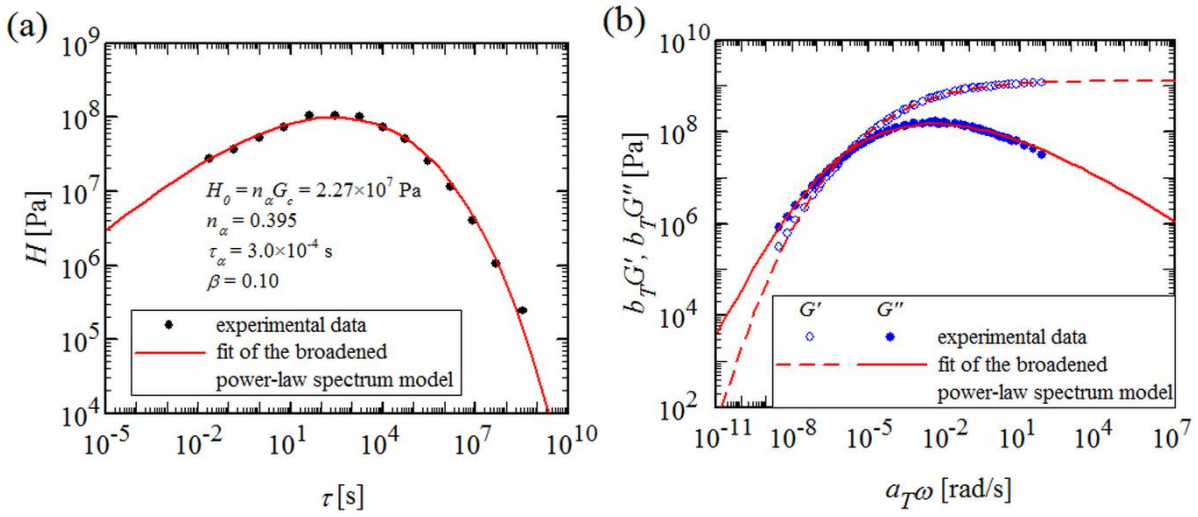

Fig. 11 Fits of the broadened power-law spectrum model, Eq. (8), to the (a) relaxation time spectrum and (b) dynamic moduli data of bitumen in the vicinity of the glass transition.

Furthermore, we suggest that the broadened power-law spectrum model can be used as a general model for describing the glassy dynamics of CGFLs, not just those of bitumen. Based on the data analyzed in this study, it appears that the power-law spectrum with a positive exponent universally describes the short-time relaxation dynamics of both SGFLs and CGFLs, and the stretched exponential part of the equation models the broadening of the glass transition dynamics in CGFLs. In particular, the stretching parameter β provides a measure of the extent of this broadening. Fig. 12 illustrates the effect of varying the value of β on various rheological material functions. As can be observed from this figure, lower values of β correspond to broader glass transition dynamics, i.e. to more complex GFLs, and vice versa. At β values greater than one, the broadened power-law spectrum model, Eq. (8), reduces to the power-law spectrum with a sharp cut-off, Eq. (2), as the stretched exponential exp[-(τ/τ_α)^β] tends quickly (1) to unity when $\tau < \tau_\alpha$ and (2) to zero when $\tau > \tau_\alpha$. Some phenomenological evidence of the general applicability of the broadened power-law spectrum model to describe the dynamics of CGFLs is presented in the Discussion section.

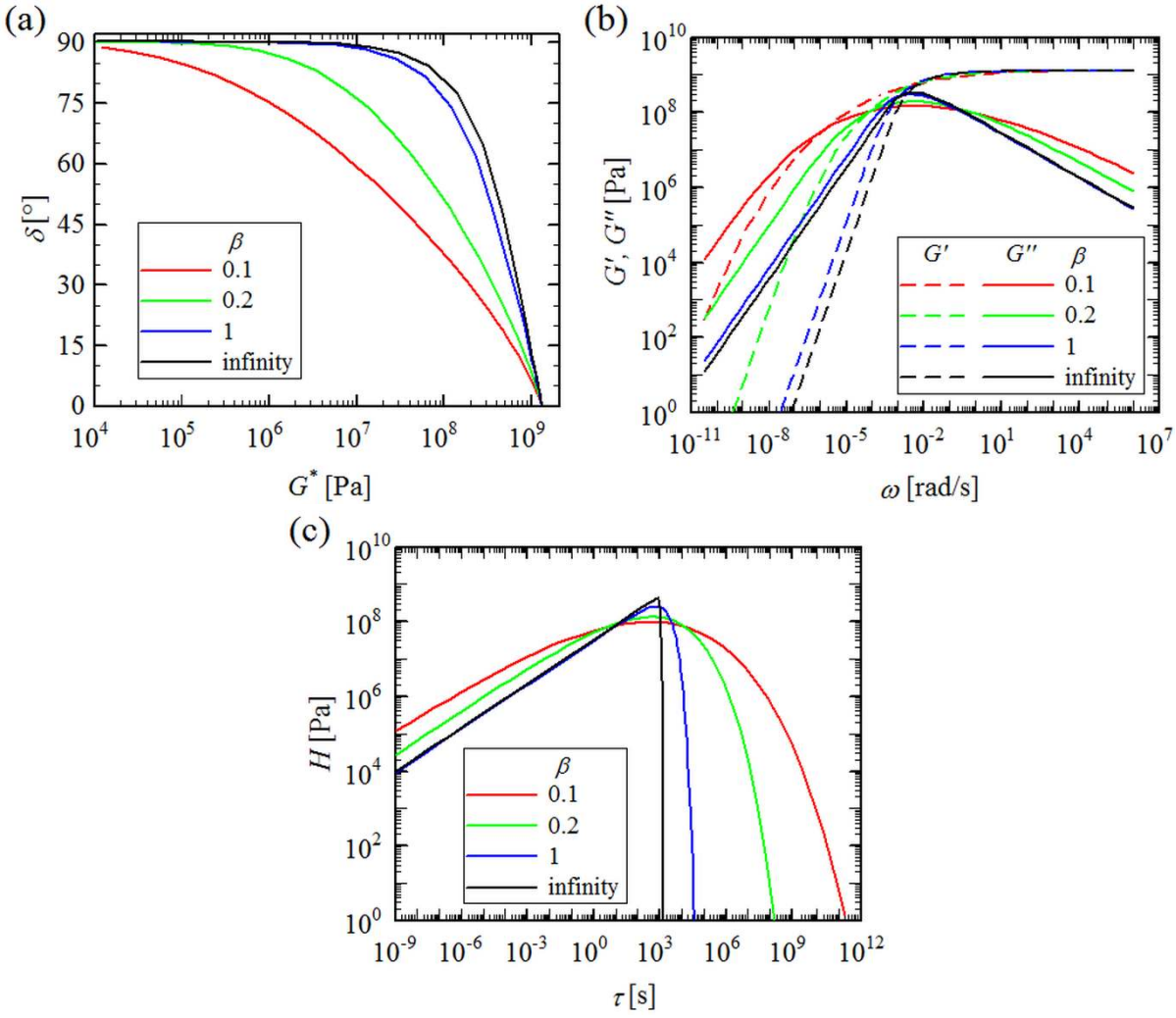

Fig. 12 Evolution in rheological material functions with varying β value as expressed by the (a) Booij-Palmen plot, (b) dynamic moduli master curves and (c) relaxation time spectrum. β = infinity corresponds to the power-law spectrum with a sharp cut-off, Eq. (2).

Discussion

The results of this study demonstrate an unusually broad glass transition in bitumen, as evidenced both by rheological and DSC measurements. Specifically, the broad glass transition dynamics manifest themselves as the wide distribution of slow relaxation modes. These observations may be attributed to the extremely complex chemical composition and structure of bitumen. In particular, different chemical components of bitumen have different T_gs. For example, Masson et al. (2005) observed four distinct glass transitions in bitumen by temperature-modulated differential scanning calorimetry, corresponding to different molecular components of bitumen. The main glass transition of bitumen, observed in Fig. 1 around -20 °C, is associated with the glass transition of alkylated cyclopentanes and cyclohexanes. In addition, observations obtained by cryogenic atomic force microscopy and phase detection microscopy have confirmed that a gradual freezing-in takes place in bitumen over a very wide temperature range upon cooling (Masson et al. 2007). It is therefore this heterogeneous freezing

of different chemical components, i.e. the effective coexistence of liquid and glassy micro-phases, that is presumed to underlie the broadened glass transition dynamics of bitumen. Alternatively, analogously to the interpretation of Rossiter et al. (see Figure 2 in Rossiter et al. 2012), it can be said that the broad glass transition of bitumen results from the superposition of the narrow glass transitions of different molecular components of bitumen.

Most surprising is the applicability of TTSP to temperatures much below the nominal glass transition temperature of T_g = -20 °C. The shape of the dynamic moduli curves does not change for temperatures between 70 and -40 °C. This is a most astounding property of bitumen. The only difference is the type of shift factor function which changes character and shows an inflection point as noticed by Kaelble (1985).

We expect that broad glass transition dynamics are a general feature of CGFLs, and the broadened power-law spectrum model, Eq. (8), is universally valid for them. Empirical evidence supporting this generalization can be found from the literature; for example, the rheological properties of DGEBA/SiO2 suspensions reported by Dannert et al. (2014) can be fairly well described by the broadened power-law spectrum model near the glass transition temperature of the DGEBA matrix. Similarly, the broadened power-law spectrum model fits well to the linear viscoelastic data reported by Liang et al. (2016) for hectorite clay suspensions during various stages of aging. Further experimental data demonstrating the general applicability of this model to various CGFLs will be presented in our forthcoming publication.

It is also important to compare the broadened power-law spectrum model with the existing models for glassy relaxation. The shape of the stretched exponential relaxation modulus of the KWW function, Eq. (1), and therefore also the shape of the corresponding relaxation time spectrum, is fully determined by a single parameter – the KWW exponent β_{KWW}. This is demonstrated in Fig. 13 where the relaxation time spectra corresponding to the KWW dynamic moduli fits of Fig. 9 have been calculated from the series expansion derived by Lindsey and Patterson (1980):

$$H(\tau) = -\frac{G_g}{\pi u}\sum_{k=1}^{\infty}\frac{(-1)^k}{k!}\sin(\pi\beta_{KWW}k)\,\Gamma(\beta_{KWW}k+1)u^{(\beta_{KWW}k+1)}, \quad \text{with } u=\frac{\tau}{\tau_{KWW}} \qquad (9)$$

Although the general shape of the KWW spectrum is similar to the broadened power-law spectrum at appropriate values of the β_{KWW} parameter, i.e. power-law behavior at short relaxation times and a broad decay at long relaxation times, it is obvious that the whole bitumen spectrum cannot be described with a single KWW fit (cf. Fig. 9). The advantage of the broadened power-law spectrum model as compared to the KWW function is that the shape of the spectrum is described by different parameters at short and long relaxation times; n_α equals the slope at short times while the breadth of the long-time decay is determined by the β parameter. This extra flexibility of the broadened power-law spectrum model is crucial in accurately describing the relaxation dynamics of CGFLs, as visualized in Fig. 13.

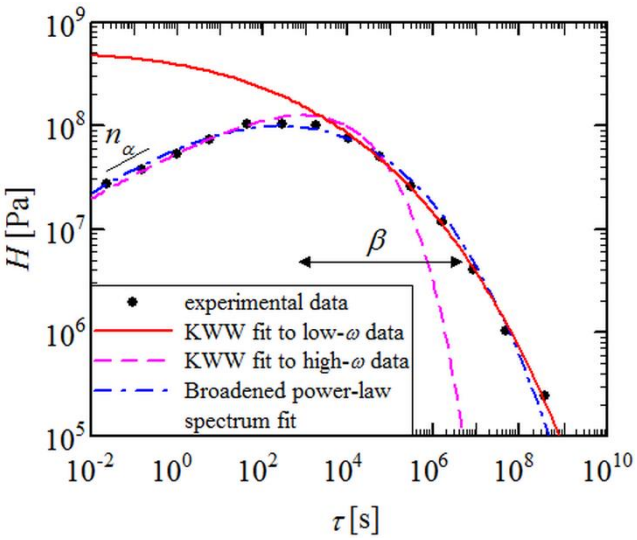

Fig. 13 Comparison of the KWW and the broadened power-law relaxation time spectra. The KWW relaxation time spectra correspond to the dynamic moduli fits of Fig. 9 and the broadened power-law spectrum fit is the same as shown in Fig. 11(a). The parameters n_α and β describe the shape of the broadened power-law spectrum at short and long relaxation times, respectively.

In addition, the Havriliak-Negami (H-N) model (1966; 1967) and its special cases the Cole-Cole (C-C) model (1941) and the Cole-Davidson (C-D) model (1951; 1950) are frequently used to describe the dynamics of GFLs. The relaxation time spectra corresponding to these models have been derived by the respective authors, with a modification to the H-N spectrum proposed by Zorn (1999):

$$H(\tau) = \frac{G_g}{\pi} \frac{y^{\alpha\beta} \sin \beta\theta}{(y^{2\alpha} + 2y^{\alpha} \cos \alpha\pi + 1)^{\beta/2}}$$

with $y = \frac{\tau}{\tau_0}$ and

$\theta = \arctan\left(\frac{\sin \alpha\pi}{y^{\alpha} + \cos \alpha\pi}\right)$ if the argument of the arctangent is positive or

$\theta = \arctan\left(\frac{\sin \alpha\pi}{y^{\alpha} + \cos \alpha\pi}\right) + \pi$ if the argument of the arctangent is negative

$$(\mathrm{H-N\ model}) \quad (10)$$

$$H(\tau) = \frac{G_g}{2\pi} \frac{\sin \alpha\pi}{\cosh[(1-\alpha) \ln y] - \cos \alpha\pi}$$

with $y = \frac{\tau}{\tau_0}$

$$(\mathrm{C-C\ model}) \quad (11)$$

$$H(\tau) = G_g \frac{\sin \beta\pi}{\pi} \left(\frac{\tau}{\tau_0 - \tau}\right)^{\beta} \quad \text{for } \tau < \tau_0$$

$$H(\tau) = 0 \quad \text{for } \tau > \tau_0 \qquad (\mathrm{C-D\ model}) \quad (12)$$

Characteristic shapes of these spectral functions are depicted in Fig. 14. It is easy to see that only the relaxation time spectrum corresponding to the general H-N model appears at least qualitatively similar in shape to the broadened power-law spectrum of bitumen. However, it should be noted that the transition from the short-time power-law behavior to the long-time decay of relaxation modes is not very well described by the H-N spectrum. It can therefore be concluded that none of the classical models described above bears a significant resemblance to the bitumen spectrum, highlighting the uniqueness of the broadened power-law spectrum model to describe the glassy dynamics of CGFLs.

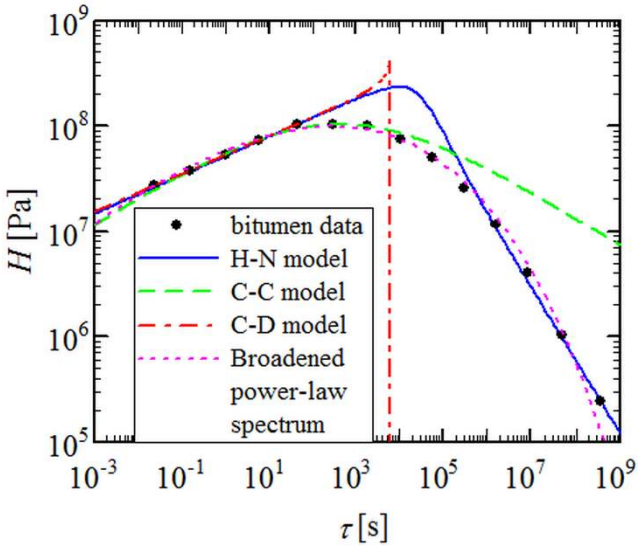

Fig. 14 Comparison of the broadened power-law spectrum with the relaxation time spectra corresponding to the Havriliak-Negami (H-N), Cole-Cole (C-C) and Cole-Davidson (C-D) models.

Although bitumen can be considered as a convenient model material for the purposes of this study, it does not allow conclusions to be drawn about the exact relationships between its chemical and microstructural properties and the broadening of the glass transition dynamics. This is because bitumen exhibits various forms of complexity as a glass-forming material. In addition to its complexity in terms of the chemical composition, bitumen has been found to micro-phase separate upon cooling through the glass transition regime. This phase separation is presumably induced by the differences in the T_gs of different molecular components of bitumen as proposed by Masson et al. (2007). The results of this study, however, are not extensive enough to determine the effect of the micro-phase separation on the broadening of the glassy dynamics, but further studies on more well-defined material systems are necessary to accomplish this.

Finally, it is noted that broad glass transition is not an unusual material property. Many material systems, such as gradient copolymers (Kim et al. 2006; Mok et al. 2008; Mok et al. 2009; Wong et al. 2007), proteins (Johari and Sartor 1998; Katayama et al. 2008; Khodadadi et al. 2010; Rouilly et al. 2001), interpenetrating polymer networks (Akay and Rollins 1993; Sperling et al. 1973; Sperling and Fay 1991), thin polymer films (Efremov et al. 2003; Forrest and Dalnoki-Veress 2001; Fukao and Miyamoto 2000; Fukao and Miyamoto 2001), shape-memory polymers (Miaudet et al. 2007; Xie 2010) and polymer blends (Lodge and McLeish 2000; Miwa et al. 2005; Sauer and Hsiao 1993; Shi et al. 2013), have been reported to exhibit this characteristic. It would be therefore interesting to test whether the broadened power-law spectrum model is applicable to all these types of materials in the vicinity of the glass transition. However, this is beyond the scope of this paper and remains an open question for future research.

Conclusion

We investigated rheological characteristics of CGFLs using bitumen as a model material. Compared to the rheological response of SGFLs, a distinct broadening of glass transition dynamics is observed in bitumen. This is manifested as a wide distribution of relaxation times which can be described by the broadened power-law spectrum model proposed in this paper. In this constitutive equation, the distribution of long relaxation modes is modeled by a stretched exponential cut-off, with parameter β serving as a measure of the broadness of the distribution. This characteristic shape of the relaxation time spectrum of bitumen is attributed to the heterogeneous glass transition behavior of this material, i.e. to the wide dispersion of glass transition temperatures among different molecular components of bitumen. As this type of heterogeneity with respect to glass transition properties is a generic feature of CGFLs, it is expected that the broadened power-law spectrum model is universally applicable to describe their glass transition dynamics. Experimental evidence supporting this generalization can be found from the literature and will be presented in our forthcoming publication. Future studies are recommended to determine the applicability of the broadened power-law spectrum model in a wide variety of material systems exhibiting broad glass transition.

Acknowledgments

O.V.L. thanks the Vilho, Yrjö, and Kalle Väisälä Foundation and Nynas AB for financial support. The authors also gratefully acknowledge technical support from Malvern Instruments Ltd. The rheological data of sucrose benzoate, *m*-toluidine and glycerol were kindly provided by Prof. Gregory McKenna (Texas Tech), and the rheological data of tetraphenyl-tetramethyl-trisiloxane (DC704), 1,2-propanediol and pentaphenyl-trimethyl-trisiloxane (DC705) were retrieved from the data repository of the Glass and Time group at Roskilde University (http://glass.ruc.dk/data/).

References

Akay M, Rollins S (1993) Transition Broadening and WLF Relationship in Polyurethane/Poly (Methyl Methacrylate) Interpenetrating Polymer Networks. Polymer 34(5):967-971

Angell CA, Ngai KL, McKenna GB, McMillan PF, Martin SW (2000) Relaxation in Glassforming Liquids and Amorphous Solids. J Appl Phys 88(6):3113-3157

Angell C, Richards B, Velikov V (1999) Simple Glass-Forming Liquids: Their Definition, Fragilities, and Landscape Excitation Profiles. J Phys Condens Matter 11(10A):A75

Baumgaertel M, Winter HH (1992) Interrelation between Continuous and Discrete Relaxation Time Spectra. J Non Newtonian Fluid Mech 44:15-36

Baumgaertel M, Schausberger A, Winter HH (1990) The Relaxation of Polymers with Linear Flexible Chains of Uniform Length. Rheol Acta 29(5):400-408

Baumgaertel M, Winter HH (1989) Determination of Discrete Relaxation and Retardation Time Spectra from Dynamic Mechanical Data. Rheol Acta 28(6):511-519

Bengtzelius U, Gotze W, Sjolander A (1984) Dynamics of Supercooled Liquids and the Glass Transition. J Phys C 17(33):5915-5934

Berry GC, Plazek DJ (1997) On the use of Stretched-Exponential Functions for both Linear Viscoelastic Creep and Stress Relaxation. Rheol Acta 36(3):320-329

Böhmer R, Ngai K, Angell C, Plazek D (1993) Nonexponential Relaxations in Strong and Fragile Glass Formers. J Chem Phys 99(5):4201-4209

Booij HC, and Palmen JHM (1992) Linear Viscoelastic Properties of Melts of Miscible Blends of Poly (Methylmethacrylate) with Poly (Ethylene Oxide). In: Moldenaers P and Keunings R (ed) Theoretical and Applied Rheology, Elsevier, Brussels, pp. 321-323

Christensen T, Olsen NB (1995) A Rheometer for the Measurement of a High Shear Modulus Covering More than Seven Decades of Frequency Below 50 kHz. Rev Sci Instrum 66(10):5019-5031

Cole KS, Cole RH (1941) Dispersion and Absorption in Dielectrics I. Alternating Current Characteristics. J Chem Phys 9(4):341-351

Dannert R, Sanctuary R, Thomassey M, Elens P, Krüger JK, Baller J (2014) Strain-Induced Low-Frequency Relaxation in Colloidal DGEBA/SiO2 Suspensions. Rheol Acta 53(9):715-723

Davidson DW, Cole RH (1951) Dielectric Relaxation in Glycerol, Propylene Glycol, and N-propanol. J Chem Phys 19(12):1484-1490

Davidson D, Cole R (1950) Dielectric Relaxation in Glycerine. J Chem Phys 18(10):1417-1417

1 Dealy J, Plazek D (2009) Time-Temperature Superposition—a Users Guide. Rheol Bull
2 78(2):16-31

3 Donth E (2001) The Glass Transition: Relaxation Dynamics in Liquids and Disordered
4 Materials, Springer, Berlin, Germany

5 Dyre JC (2006) Colloquium: The Glass Transition and Elastic Models of Glass-Forming
6 Liquids. Rev Mod Phys 78(3):953-972

7 Efremov MY, Olson EA, Zhang M, Zhang Z, Allen LH (2003) Glass Transition in Ultrathin
8 Polymer Films: Calorimetric Study. Phys Rev Lett 91(8):085703

9 Elmatad YS, Chandler D, Garrahan JP (2009) Corresponding States of Structural Glass
10 Formers. J Phys Chem B 113:5563-5567

11 Elmatad Y, Chandler D, Garrahan J (2010) Corresponding States of Structural Glass
12 Formers. II. J Phys Chem B 114(51):17113-17119

13 Eschrich H (1980) Properties and Long-Term Behaviour of Bitumen and Radioactive Waste-
14 Bitumen Mixtures, Svensk Karnbransleforsorjning AB/Projekt Karnbranslesakerhet,

15 Ferry JD (1980) Viscoelastic Properties of Polymers, John Wiley & Sons, New York

16 Forrest JA, Dalnoki-Veress K (2001) The Glass Transition in Thin Polymer Films. Adv
17 Colloid Interface Sci 94(1):167-195

18 Friedrich C, Braun H (1992) Generalized Cole-Cole Behavior and its Rheological Relevance.
19 Rheol Acta 31(4):309-322

20 Fukao K, Miyamoto Y (2001) Slow Dynamics Near Glass Transitions in Thin Polymer
21 Films. Phys Rev E Stat Nonlin Soft Matter Phys 64(1):011803

22 Fukao K, Miyamoto Y (2000) Glass Transitions and Dynamics in Thin Polymer Films:
23 Dielectric Relaxation of Thin Films of Polystyrene. Phys Rev E Stat Nonlin Soft Matter Phys
24 61(2):1743

25 Götze W, Sjögren L (1992) Relaxation Processes in Supercooled Liquids. Rep Prog Phys
26 55(3):241-370

27 Götze W (1999) Recent Tests of the Mode-Coupling Theory for Glassy Dynamics. J Phys
28 Condens Matter 11(10A):A1-A45

29 Hansen C, Stickel F, Richert R, Fischer EW (1998) Dynamics of Glass-Forming Liquids. IV.
30 True Activated Behavior Above 2 GHz in the Dielectric A-Relaxation of Organic Liquids. J
31 Chem Phys 108(15):6408-6415

32 Hansen C, Stickel F, Berger T, Richert R, Fischer EW (1997) Dynamics of Glass-Forming
33 Liquids. III. Comparing the Dielectric A-and B-Relaxation of 1-Propanol and O-Terphenyl. J
34 Chem Phys 107(4):1086-1093

Havriliak S, Negami S (1967) A Complex Plane Representation of Dielectric and Mechanical Relaxation Processes in some Polymers. Polymer 8:161-210

Havriliak S, Negami S (1966) A Complex Plane Analysis of A-dispersions in some Polymer Systems. J Polym Sci C 14(1):99-117

Hecksher T, Olsen NB, Nelson KA, Dyre JC, Christensen T (2013) Mechanical Spectra of Glass-Forming Liquids. I. Low-Frequency Bulk and Shear Moduli of DC704 and 5-PPE Measured by Piezoceramic Transducers. J Chem Phys 138(12):12A543

Hecksher T, Nielsen AI, Olsen NB, Dyre JC (2008) Little Evidence for Dynamic Divergences in Ultraviscous Molecular Liquids. Nature Phys 4(9):737-741

Hutcheson S, McKenna G (2008) The Measurement of Mechanical Properties of Glycerol, M-Toluidine, and Sucrose Benzoate Under Consideration of Corrected Rheometer Compliance: An in-Depth Study and Review. J Chem Phys 129(7):074502

Igarashi B, Christensen T, Larsen EH, Olsen NB, Pedersen IH, Rasmussen T, Dyre JC (2008) A Cryostat and Temperature Control System Optimized for Measuring Relaxations of Glass-Forming Liquids. Rev Sci Instrum 79(4):045105

Johari G, and Sartor G (1998) Thermodynamic and Kinetic Features of Vitrification and Phase Transformations of Proteins and Other Constituents of Dry and Hydrated Soybean, a High Protein Cereal. In: Reid DS (ed) The Properties of Water in Foods ISOPOW 6, Springer, pp. 103-138

Kaelble DH (1985) Computer Aided Design of Polymers and Composites, Marcel Dekker, New York, NY, pp. 145-147

Katayama DS, Carpenter JF, Manning MC, Randolph TW, Setlow P, Menard KP (2008) Characterization of Amorphous Solids with Weak Glass Transitions using High Ramp Rate Differential Scanning Calorimetry. J Pharm Sci 97(2):1013-1024

Khodadadi S, Malkovskiy A, Kisliuk A, Sokolov A (2010) A Broad Glass Transition in Hydrated Proteins. Biochim Biophys Acta, Proteins Proteomics 1804(1):15-19

Kim J, Mok MM, Sandoval RW, Woo DJ, Torkelson JM (2006) Uniquely Broad Glass Transition Temperatures of Gradient Copolymers Relative to Random and Block Copolymers Containing Repulsive Comonomers. Macromolecules 39(18):6152-6160

Kohlrausch R (1854) Theorie Des Elektrischen Rückstandes in Der Leidener Flasche. Ann Phys (Berlin) 167(2):179-214

Langer JS (2007) The Mysterious Glass Transition. Phys Today 60(2):8-9

Laukkanen OV (2017) Small-Diameter Parallel Plate Rheometry: A Simple Technique for Measuring Rheological Properties of Glass-Forming Liquids in Shear. Rheol Acta 56:661-671

Le Bourhis E (2008) Glass Rheology. In: Le Bourhis E (ed) Glass: Mechanics and Technology, Wiley-VCH Verlag GmbH & Co. KGaA, Weinheim, Germany, pp. 83-134

Lesueur D (2009) The Colloidal Structure of Bitumen: Consequences on the Rheology and on the Mechanisms of Bitumen Modification. Adv Colloid Interface Sci 145(1):42-82

Lesueur D (1999) Letter to the Editor: On the Thermorheological Complexity and Relaxation Modes of Asphalt Cements. J Rheol 43(6):1701-1704

Lesueur D, Gerard J, Claudy P, Letoffe J, Planche J, Martin D (1996) A Structure-related Model to Describe Asphalt Linear Viscoelasticity. J Rheol 40(5):813-836

Liang C, Sun W, Wang T, Liu X, Tong Z (2016) Rheological Inversion of the Universal Aging Dynamics of Hectorite Clay Suspensions. Colloids Surf Physicochem Eng Aspects 490:300-306

Lindsey C, Patterson G (1980) Detailed Comparison of the Williams–Watts and Cole–Davidson Functions. J Chem Phys 73(7):3348-3357

Lodge TP, McLeish TC (2000) Self-Concentrations and Effective Glass Transition Temperatures in Polymer Blends. Macromolecules 33(14):5278-5284

Lunkenheimer P, Schneider U, Brand R, Loid A (2000) Glassy Dynamics. Contemp Phys 41(1):15-36

Maggi C, Jakobsen B, Christensen T, Olsen NB, Dyre JC (2008) Supercooled Liquid Dynamics Studied Via Shear-Mechanical Spectroscopy. J Phys Chem B 112(51):16320-16325

Marin G (1988) Oscillatory Rheometry. In: Collyer AA and Clegg DW (ed) Rheological Measurements, Elsevier, London, UK, pp. 297-343

Masson J, Leblond V, Margeson J, Bundalo-Perc S (2007) Low-temperature Bitumen Stiffness and Viscous Paraffinic Nano-and Micro-domains by Cryogenic AFM and PDM. J Microsc 227(3):191-202

Masson J, Polomark G, Collins P (2005) Glass Transitions and Amorphous Phases in SBS–bitumen Blends. Thermochim Acta 436(1):96-100

Mauro JC, Yue Y, Ellison AJ, Gupta PK, Allan DC (2009) Viscosity of Glass-Forming Liquids. Proc Natl Acad Sci U S A 106(47):19780-19784. 10.1073/pnas.0911705106 [doi]

McKenna GB, Zhao J (2015) Accumulating Evidence for Non-Diverging Time-Scales in Glass-Forming Fluids. J Non Cryst Solids 407:3-13

McKenna GB (2012) Physical Aging in Glasses and Composites. In: Pochiraju KV, Tandon G and Schoeppner GA (ed) Long-Term Durability of Polymeric Matrix Composites, Springer, pp. 237-309

McKenna GB (2009) A Brief Discussion: Thermodynamic and Dynamic Fragilities, Non-Divergent Dynamics and the Prigogine–Defay Ratio. J Non Cryst Solids 355(10):663-671

McKenna GB (2008) Glass Dynamics: Diverging Views on Glass Transition. Nature Phys 4(9):673-673

Miaudet P, Derre A, Maugey M, Zakri C, Piccione PM, Inoubli R, Poulin P (2007) Shape and Temperature Memory of Nanocomposites with Broadened Glass Transition. Science 318(5854):1294-1296

Mills J (1974) Low Frequency Storage and Loss Moduli of Soda-Silica Glasses in the Transformation Range. J Non Cryst Solids 14(1):255-268

Miwa Y, Usami K, Yamamoto K, Sakaguchi M, Sakai M, Shimada S (2005) Direct Detection of Effective Glass Transitions in Miscible Polymer Blends by Temperature-Modulated Differential Scanning Calorimetry. Macromolecules 38(6):2355-2361

Mok MM, Kim J, Wong CL, Marrou SR, Woo DJ, Dettmer CM, Nguyen ST, Ellison CJ, Shull KR, Torkelson JM (2009) Glass Transition Breadths and Composition Profiles of Weakly, Moderately, and Strongly Segregating Gradient Copolymers: Experimental Results and Calculations from Self-Consistent Mean-Field Theory. Macromolecules 42(20):7863-7876

Mok MM, Kim J, Torkelson JM (2008) Gradient Copolymers with Broad Glass Transition Temperature Regions: Design of Purely Interphase Compositions for Damping Applications. J Polym Sci Part B Polym Phys 46(1):48-58

Mours M, Winter H (1994) Time-Resolved Rheometry. Rheol Acta 33(5):385-397

Ngai KL, Plazek DJ, Rendell RW (1997) Some Examples of Possible Descriptions of Dynamic Properties of Polymers by Means of the Coupling Model. Rheol Acta 36(3):307-319

Pazmiño Betancourt BA, Douglas JF, Starr FW (2014) String Model for the Dynamics of Glass-Forming Liquids. J Chem Phys 140(20):204509

Plazek DJ, Magill JH (1966) Physical Properties of Aromatic Hydrocarbons. I. Viscous and Viscoelastic Behavior of 1: 3: 5-Tri-α-Naphthyl Benzene. J Chem Phys 45(8):3038-3050

Qin Q, Schabron JF, Boysen RB, Farrar MJ (2014) Field Aging Effect on Chemistry and Rheology of Asphalt Binders and Rheological Predictions for Field Aging. Fuel 121:86-94

Redelius P, Soenen H (2015) Relation between Bitumen Chemistry and Performance. Fuel 140:34-43

Richert R, Angell C (1998) Dynamics of Glass-Forming Liquids. V. on the Link between Molecular Dynamics and Configurational Entropy. J Chem Phys 108(21):9016-9026

Rossiter J, Takashima K, Mukai T (2012) Shape Memory Properties of Ionic Polymer–metal Composites. Smart Mater Struct 21(11):112002

Rouilly A, Orliac O, Silvestre F, Rigal L (2001) DSC Study on the Thermal Properties of Sunflower Proteins According to their Water Content. Polymer 42(26):10111-10117

Rowe GM, Sharrock M (2011) Alternate Shift Factor Relationship for Describing Temperature Dependency of Viscoelastic Behavior of Asphalt Materials. Trans Res Rec 2207(1):125-135

Sauer BB, Hsiao BS (1993) Broadening of the Glass Transition in Blends of Poly (Aryl Ether Ketones) and a Poly (Ether Imide) as Studied by Thermally Stimulated Currents. J Polym Sci Part B Polym Phys 31(8):917-932

Schröter K, Hutcheson S, Shi X, Mandanici A, McKenna G (2006) Dynamic Shear Modulus of Glycerol: Corrections due to Instrument Compliance. J Chem Phys 125(21):214507

Schröter K, Donth E (2000) Viscosity and Shear Response at the Dynamic Glass Transition of Glycerol. J Chem Phys 113(20):9101-9108

Shi P, Schach R, Munch E, Montes H, Lequeux F (2013) Glass Transition Distribution in Miscible Polymer Blends: From Calorimetry to Rheology. Macromolecules 46(9):3611-3620

Soenen H, Lu X, Laukkanen O (2016) Oxidation of Bitumen: Molecular Characterization and Influence on Rheological Properties. Rheol Acta 55(4):315-326

Soenen H, Redelius P (2014) The Effect of Aromatic Interactions on the Elasticity of Bituminous Binders. Rheol Acta 53(9):741-754

Sperling L, Fay J (1991) Factors which Affect the Glass Transition and Damping Capability of Polymers. Polym Adv Technol 2(1):49-56

Sperling L, Chiu T, Thomas D (1973) Glass Transition Behavior of Latex Interpenetrating Polymer Networks Based on Methacrylic/Acrylic Pairs. J Appl Polym Sci 17(8):2443-2455

Stadler FJ, Chen S, Chen S (2015) On “modulus Shift” and Thermorheological Complexity in Polyolefins. Rheol Acta 54(8):695-704

Stickel F, Fischer EW, Richert R (1996) Dynamics of Glass-forming Liquids. II. Detailed Comparison of Dielectric Relaxation, Dc-conductivity, and Viscosity Data. J Chem Phys 104(5):2043-2055

Stickel F, Fischer EW, Richert R (1995) Dynamics of Glass-forming Liquids. I. Temperature-derivative Analysis of Dielectric Relaxation Data. J Chem Phys 102(15):6251-6257

Struik L (1977). Physical aging in amorphous polymers and other materials. Dissertation, Delft University of Technology.

Tabatabaee HA, Velasquez R, Bahia HU (2012) Predicting Low Temperature Physical Hardening in Asphalt Binders. Constr Build Mater 34:162-169

van Gurp M, Palmen J (1998) Time-Temperature Superposition for Polymeric Blends. Rheol Bull 67(1):5-8

1 Williams G, Watts DC (1970) Non-Symmetrical Dielectric Relaxation Behaviour Arising
2 from a Simple Empirical Decay Function. Trans Faraday Soc 66:80-85

3 Winter HH (2013) Glass Transition as the Rheological Inverse of Gelation. Macromolecules
4 46(6):2425-2432

5 Winter HH, Siebenbürger M, Hajnal D, Henrich O, Fuchs M, Ballauff M (2009) An
6 Empirical Constitutive Law for Concentrated Colloidal Suspensions in the Approach of the
7 Glass Transition. Rheol Acta 48(7):747-753

8 Wong CL, Kim J, Torkelson JM (2007) Breadth of Glass Transition Temperature in
9 Styrene/Acrylic Acid Block, Random, and Gradient Copolymers: Unusual Sequence
10 Distribution Effects. J Polym Sci Part B Polym Phys 45(20):2842-2849

11 Xie T (2010) Tunable Polymer Multi-Shape Memory Effect. Nature 464(7286):267-270

12 Zanzotto L, Stastna J (1997) Dynamic Master Curves from the Stretched Exponential
13 Relaxation Modulus. J Polym Sci Part B Polym Phys 35(8):1225-1232

14 Zhao J, Simon SL, McKenna GB (2013) Using 20-Million-Year-Old Amber to Test the
15 Super-Arrhenius Behaviour of Glass-Forming Systems. Nat Commun 4:1783

16 Zorn R (1999) Applicability of Distribution Functions for the Havriliak–Negami Spectral
17 Function. J Polym Sci Part B Polym Phys 37(10):1043-1044

18

19